Supplementary Information:

Electrically Adjusted Deep-Ultraviolet/Near-Infrared Single-Band/Dual-Band Imaging Photodetectors Based on $Cs_3Cu_2I_5/PdTe_2/Ge$ Multiheterostructures

Yi Liang,[1] Chao Xie,[2] Chengyun Dong,[1] Xiaowei Tong,[1] Wenhua Yang,[1] Chunyan Wu,[1] and Linbao Luo[1*]*

[1] School of Microelectronics, Hefei University of Technology, Hefei, Anhui 230009, P. R. China

[2] School of Electronics and Information Engineering, Information Materials and Intelligent Sensing Laboratory of Anhui Province, Industry-Education-Research Institute of Advanced Materials and Technology for Integrated Circuits, Anhui University, Hefei, Anhui 230601, P. R. China

[*] Email: chaoxie@ahu.edu.cn, luolb@hfut.edu.cn

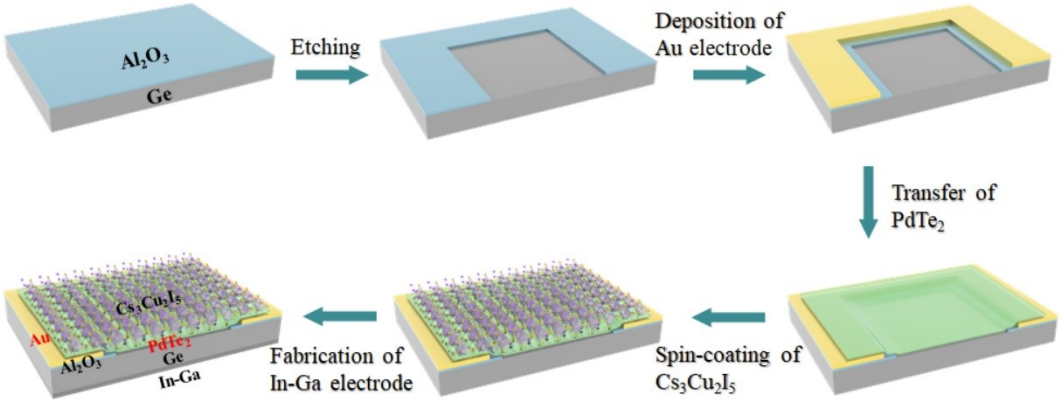

Figure S1. Schematic diagram of the procedures for fabricating $Cs_3Cu_2I_5/PdTe_2/Ge$ multiheterostructure-based photodetector.

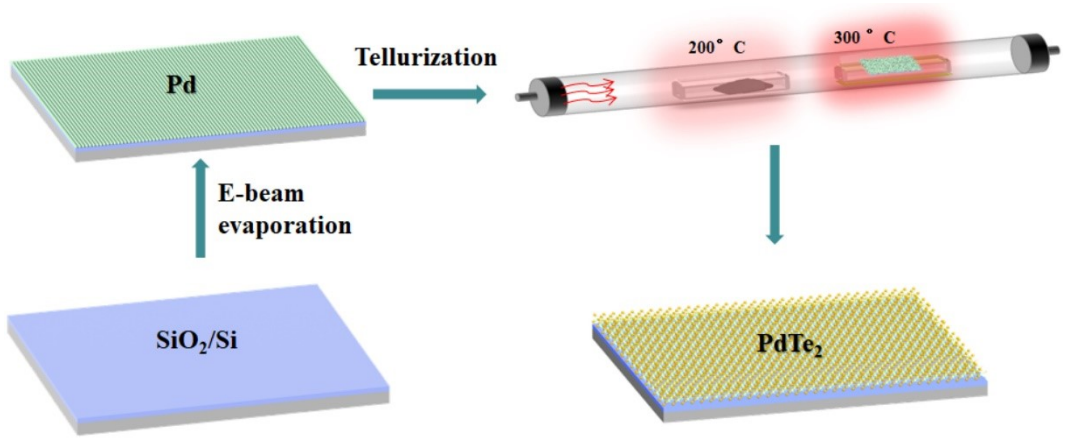

Figure S2. Schematic illustration for the synthesis of 2D $PdTe_2$ multilayer *via* a thermal-assisted tellurization approach.

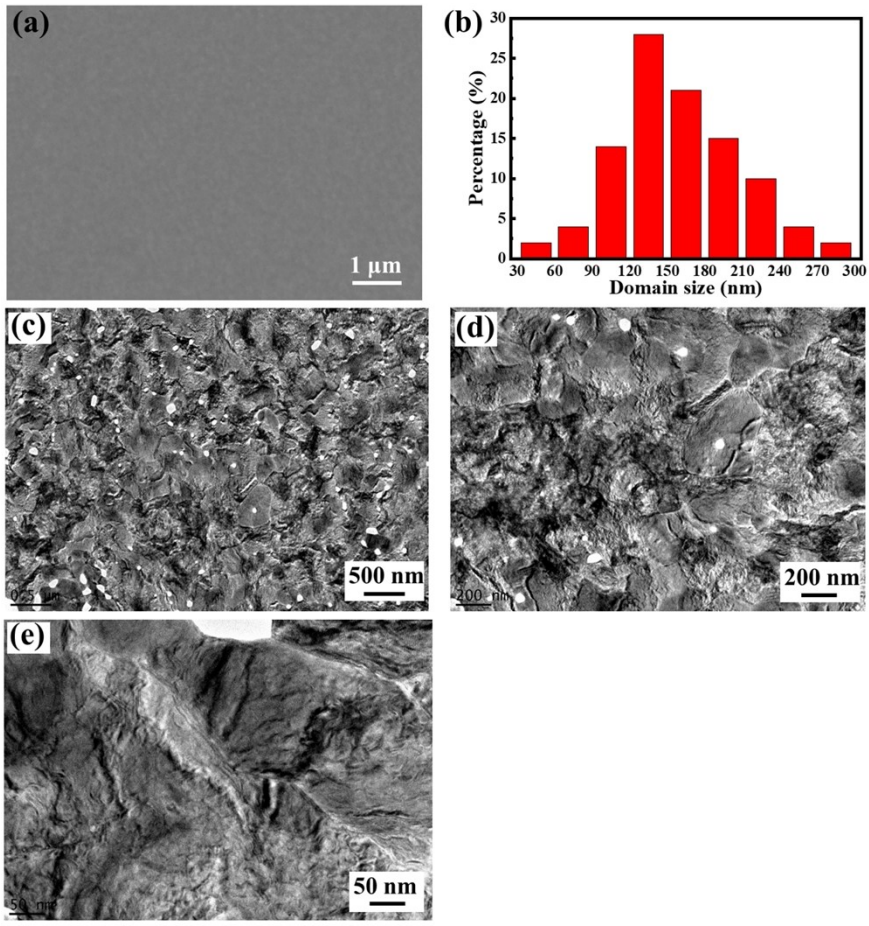

Figure S3. (a) SEM image of the 2D $PdTe_2$ multilayer on a SiO_2/Si substrate. (b) Distribution of the size of the crystalline domains of the $PdTe_2$ multilayer. (c)-(e) TEM images of the $PdTe_2$ multilayer at different magnifications.

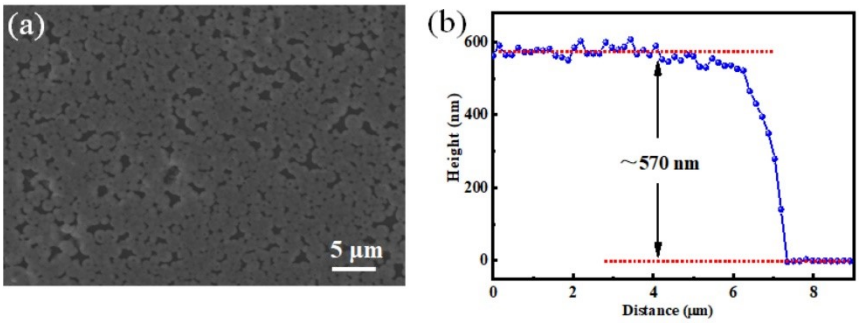

Figure S4. (a) SEM image and (b) height profile of the $Cs_3Cu_2I_5$ film.

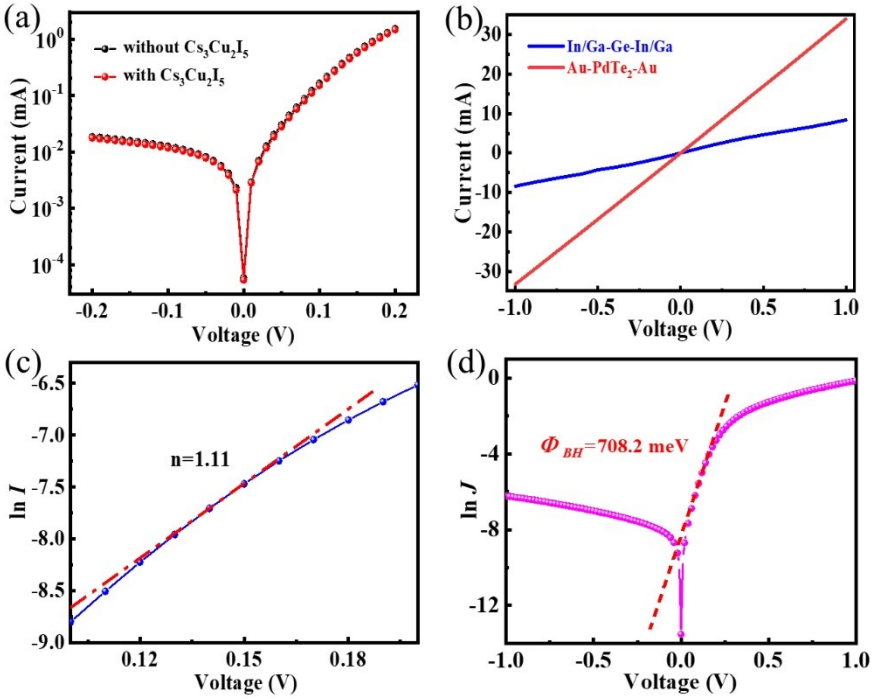

Figure S5. (a) *I-V* curves of the $PdTe_2$/Ge heterostructures without and with $Cs_3Cu_2I_5$ coating. (b) *I-V* curves of In/Ga-Ge-In/Ga and Au-$PdTe_2$-Au, indicating good ohmic contacts between Ge and In/Ga electrode, $PdTe_2$ and Au electrode. (c) ln*I-V* curve for estimating the diode ideality factor (*n*). (d) The plot of ln*J-V* curve for calculating the barrier height of the heterostructure.

The barrier height (Φ_{BH}) of the heterojunction was calculated following the thermionic emission theory. According to this theory, the diode characteristics of the heterojunction could be described by majority carriers over a zero bias Φ_{BH}, from the $PdTe_2$ to Ge:[1]

$$J(T,V) = J_S(T)\left[\exp\left(\frac{eV}{nK_BT}\right) - 1\right]$$

where e is the elementary charge, K_B is the Boltzmann constant, and T is the temperature. The

saturation current density $J_S(T)$ is given by:

$$J_S(T) = A^* T^2 exp(-\frac{e\Phi_{BH}}{K_B T})$$

where A* is the effective Richardson constant, which is 142.8 $Acm^{-2}K^{-2}$ for n-Ge.[2] By deducing the ln*J*-*V* curve in Fig. S5(d), $J_S(T)$=4.1×10^{-4} Acm^{-2} was obtained. Therefore, according to the above equations, the Φ_{BH} was calculated to be ~708.2 meV for the present heterojunction.

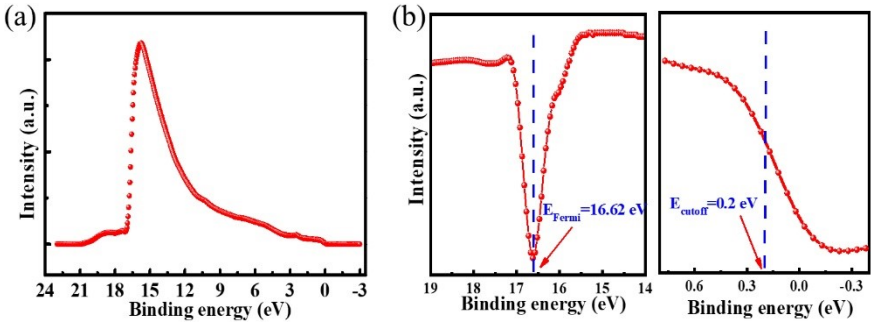

Figure S6. (a) UPS spectrum of the 2D $PdTe_2$ multilayer. (b) The differential of Fermi edge (E_{Fermi}) region (left panel) and the secondary electron cut-off edge (E_{cutoff}) (right panel) of the 2D $PdTe_2$ multilayer, showing an E_{Fermi} and E_{cutoff} levels of 16.62 eV and 0.2 eV, respectively.

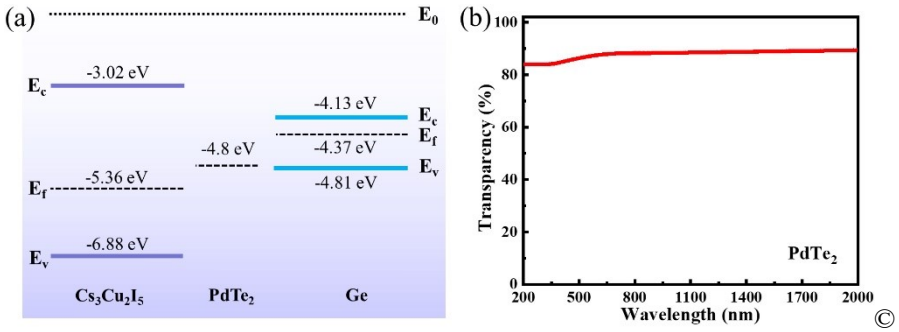

Figure S7. (a) Energy band diagram of $Cs_3Cu_2I_5$, $PdTe_2$ multilayer and Ge before contact. (b) Transparency spectrum of the ~48.3 nm thick $PdTe_2$ multilayer.

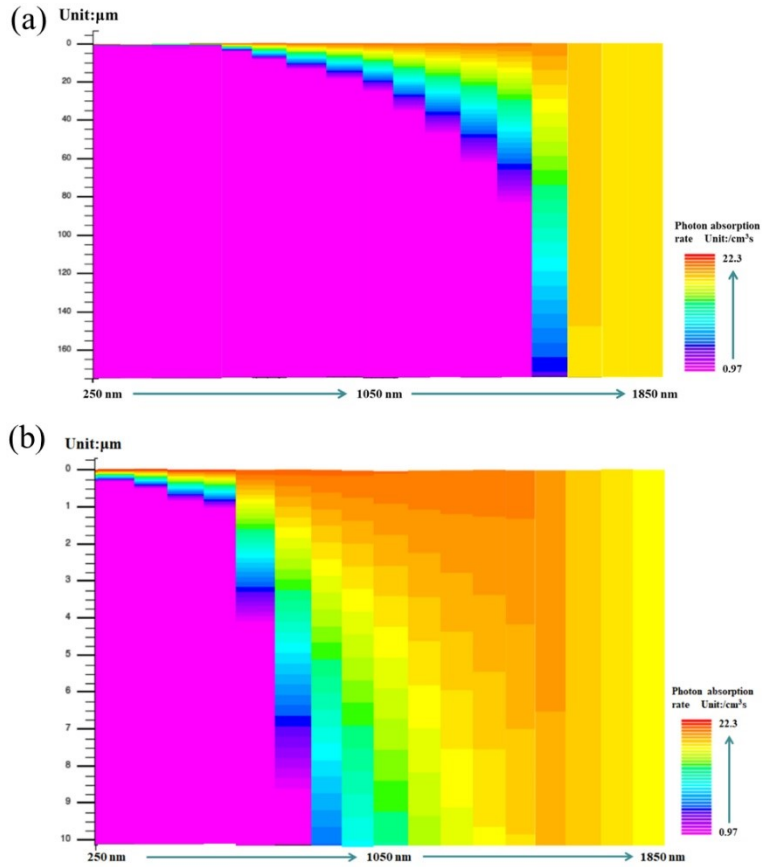

Figure S8. Contour maps of photo absorption rate as functions of incident light wavelength and depth in Ge (a) from 0 to 180 μm and (b) from 0 to 10 μm.

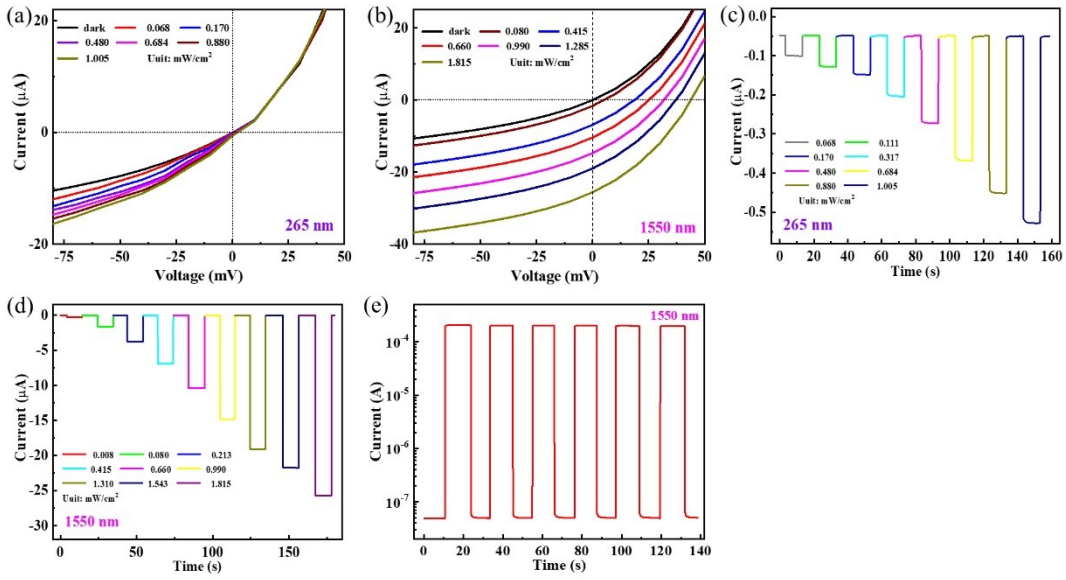

Figure S9. *I-V* curves of the photodetector under (a) 265 nm and (b) 1550 nm illuminations with different light intensities. Temporal photoresponse of the photodetector under (c) 265 nm and (d)

1550 nm illuminations with different light intensities. (e) Temporal photoresponse under 1550 nm illumination at a light intensity of 15.17 $mWcm^{-2}$.

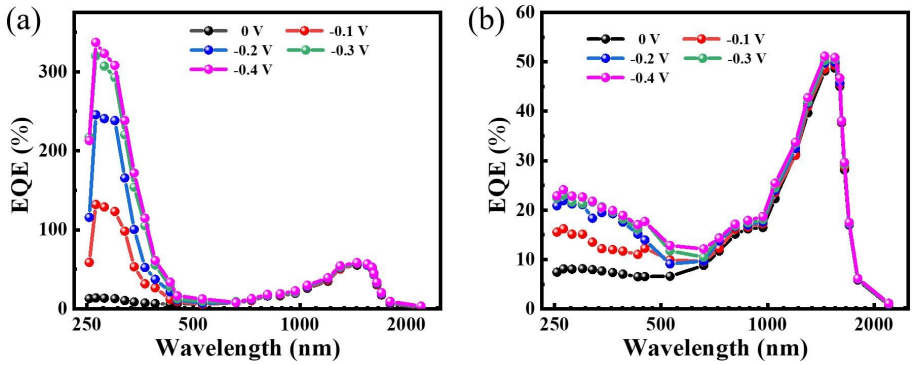

Figure S10. EQE as a function of incident light wavelength for the $PdTe_2$/Ge heterostructures (a) with and (b) without $Cs_3Cu_2I_5$ coating, at different bias voltages.

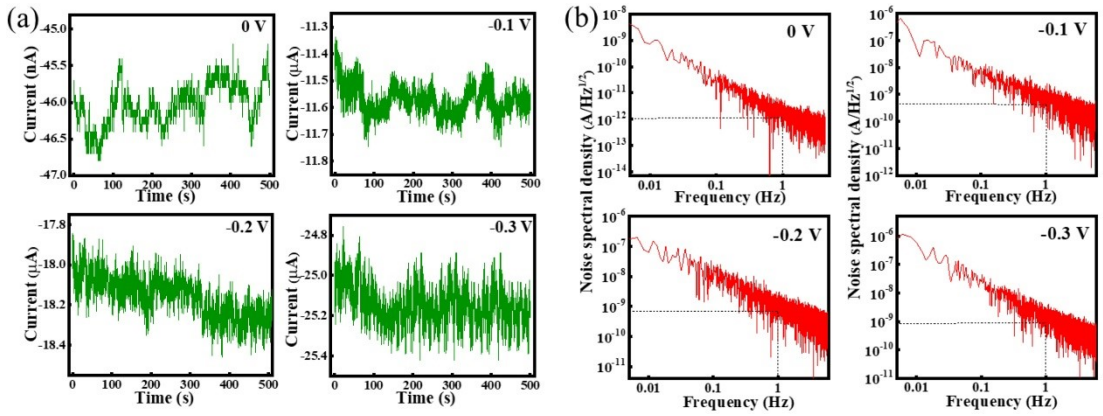

Figure S11. (a) The noise of the dark current and (b) analysis of noise spectral density of the multiheterostructure-based photodetector at different bias voltages.

The noise of the dark current of the multiheterostructure-based photodetector was recorded by using a low noise current preamplifier (Stanford Research System, Model SR570) connected with a digital oscilloscope (Tektronix, TDS 2012C). The current value of photodetector was converted into voltage signal through the low noise current preamplifier, and then collected by the oscilloscope. During the measurement, the filter of the preamplifier was set to "LOWPASS"

mode with frequency at 1000 Hz to filter high-frequency noise in ambient conditions. The noise of the dark current at different bias voltages was shown in Fig. S10(a). The noise spectral density in Fig. S10(b) was acquired by doing a Fourier transform (FFT) of the measured dark current, according to a method used in previous studies.[3,4]

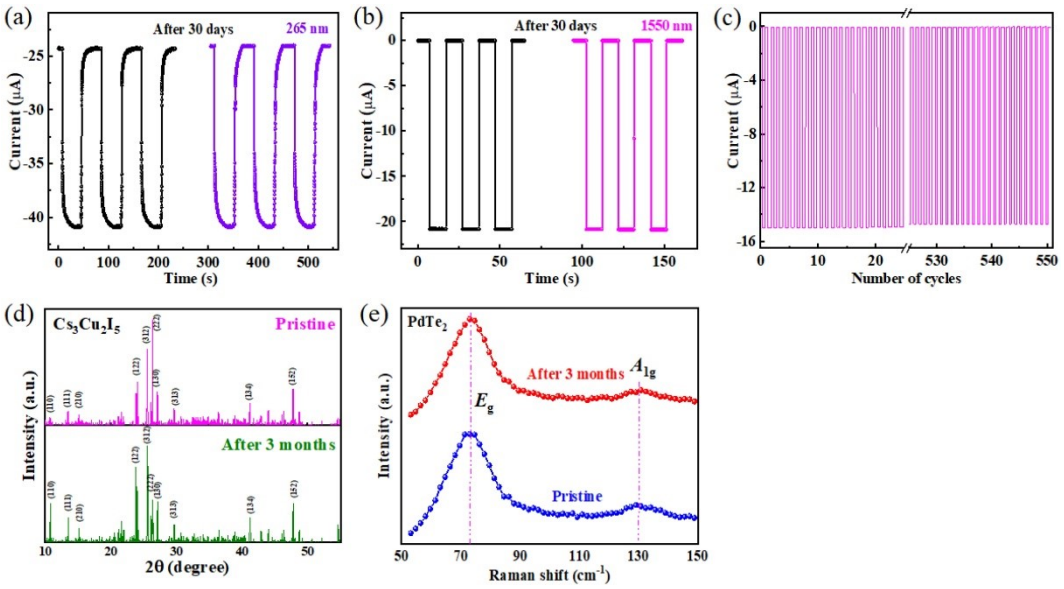

Figure S12. Temporal photoresponse of the multiheterostructure-based photodetector at (a) 265 nm and (b) 1550 nm before and after storage in ambient conditions for 30 days. (c) Temporal photoresponse over 500 hundreds of cycles of operation at 1550 nm. (d) XRD pattern of the $Cs_3Cu_2I_5$ film before and after storage in ambient conditions for 3 months. (e) Raman spectra of the 2D $PdTe_2$ multilayer before and after storage in ambient conditions for 3 months.

References

1. Shi, E. *et al.* Colloidal antireflection coating improves graphene-silicon solar cells. *Nano Lett.* **13**, 1776–1781 (2013).
2. Sze, S. M. & Ng, K. K. *Physics of Semiconductor Devices*. *Physics of semiconductor device* (2007). doi:10.1049/ep.1970.0039
3. Liu, C.-H., Chang, Y.-C., Norris, T. B. & Zhong, Z. Graphene photodetectors with ultra-broadband and high responsivity at room temperature. *Nat. Nanotechnol.* **9**, 273–278 (2014).
4. Fang, Y., Armin, A., Meredith, P. & Huang, J. Accurate characterization of next-generation thin-film photodetectors. *Nat. Photonics* **13**, 1–4 (2019).